

# Compensating Frequency Drift in DPSK Systems via Baseband Signal Processing

Zae Yong Choi and Yong Hoon Lee

**Abstract**— A new baseband signal processing method for compensating frequency shift in differential phase-shift keying (DPSK) systems is introduced. This method consists of a signal processor for the initial acquisition of frequency shift and a simple adaptive equalizer for tracking. The former is based on the observation that the effect of frequency shift can be eliminated by using *boundary* values of the received baseband signal between symbol periods. The latter is a single tap equalizer employing the least mean-square (LMS) adaptation algorithm. Computer simulation results demonstrate that the proposed frequency shift compensation technique outperforms existing methods, and works well for a wide range of frequency shift.

## I. INTRODUCTION

IN DIFFERENTIAL phase-shift keying (DPSK), the performance of noncoherent detection severely degrades if the carrier frequency at the receiver deviates from its original value due to either limited oscillator precision or the Doppler effect [1]–[3]. One common way of dealing with this limitation is to employ an automatic frequency control (AFC) loop which operates on a preamble [4]. The use of such an AFC loop, however, may not be recommended in some applications where data are transmitted in bursts, as in time-division multiple-access (TDMA) systems, because the preamble for AFC may take a significant portion of the burst interval. For such applications, some alternative methods that can correct frequency offset without the preamble have been developed: a technique which estimates the phase shift by observing the phase change over half a symbol within each symbol interval was proposed in [5], one-tap adaptive equalizers correcting the frequency drift at baseband were proposed in [6]–[8], and techniques estimating the frequency offset from the  $M$ th power of a baseband signal in  $M$ -ary DPSK were proposed in [11], [12]. These techniques have been shown to be useful for compensating some frequency shift, and are simpler to implement than conventional AFC; however, their performance rapidly degrades as the frequency shift increases.

In this paper, we introduce a new baseband signal processing method that can correct a much heavier frequency shift by incorporating the adaptive equalizer in [6] together with a novel acquisition scheme. The latter is based upon realizing that the effect of the frequency shift can be eliminated by using *boundary* values of the received baseband signal between symbol periods when rectangular pulses are transmitted. Thus, after converting each received pulse into a rectangular-shaped

Paper approved by M. Luise, the Editor for Synchronization of the IEEE Communications Society. Manuscript received June 25, 1996; revised September 3, 1996. This paper was presented in part at MILCOM'96, McLean, VA, October 21–24, 1996.

The authors are with the Department of Electrical Engineering, Korea Advanced Institute of Science and Technology, Yusong-gu, Taejeon, 305-701, Korea.

Publisher Item Identifier S 0090-6778(97)05740-1.

one, we estimate such boundary values from the Nyquist rate (twice the symbol rate) samples of received baseband signals, and use them for the initial acquisition of frequency shift. It will be shown through simulation that the proposed frequency shift compensation technique outperforms existing methods, and performs well for a wide range of frequency shift.

## II. FREQUENCY SHIFT COMPENSATION USING AN EQUALIZER

In this section we briefly review the compensation method in [6]. Suppose that the input to the receiver shown in Fig. 1 is a frequency-shifted DPSK signal expressed as

$$s(t) = \sqrt{2E_s/T} \cos\{(\omega_0 + \Delta\omega)t + \theta(t) + \theta_0\} \quad (1)$$

where  $E_s$  and  $T$  denote the symbol energy and duration, respectively,  $\Delta\omega = 2\pi\Delta f$  is the frequency shift in radians,  $\Delta f < (1/T)$ ,  $\theta(t)$  is  $M$ -ary DPSK modulation with symbol rate  $1/T$ , and  $\theta_0$  is the initial phase. Here, for the time being, we assume that the channel is ideal—the received signal  $s(t)$  is noise free and there is no multipath fading. The input  $x_n$  to the decision device in Fig. 1 is expressed as

$$x_n = d_n \cdot e^{j\Delta\omega T} \quad (2)$$

where  $d_n = e^{j(\theta_n - \theta_{n-1})}$  and  $\theta_n = \theta(nT)$ . For the binary case,  $\theta_n - \theta_{n-1}$  is either 0 or  $\pi$ , and the worst case occurs when  $\Delta\omega T = \pi$ . The one-tap adaptive equalizer in [6], called the *feedback-frequency drift compensator* (FB-FDC), correcting the effect of  $\Delta f$  is shown in Fig. 2. The input to the decision device denoted by  $y_n$  in Fig. 2 is given by

$$y_n = x_n \cdot \hat{W}_n^* \quad (3)$$

where

$$\hat{W}_n^* = (1 - \alpha)\hat{W}_{n-1}^* + \alpha x_{n-1}^* \hat{d}_{n-1}; \quad (4)$$

$0 < \alpha < 1$ ,  $\hat{W}_n$  and  $\hat{d}_n$  are the estimates of  $e^{j\Delta\omega T}$  and  $d_n$ , respectively, at time  $n$ , and  $*$  denotes the complex conjugate. This equalizer was designed to minimize the mean-squared error between  $d_n$  and  $y_n$ . Note that  $y_n = d_n$  when  $\hat{W}_n = e^{j\Delta\omega T}$  since  $|e^{j\Delta\omega T}| = 1$ . The tap adaptation in (4) is, in fact, a *least mean-square* (LMS) algorithm [9]. Due to the lack of a training sequence, this equalizer works well only when  $\Delta f$  is small.

## III. DETECTION THROUGH BOUNDARY-VALUE ESTIMATION

### A. Rectangular Pulse Case

Suppose that at the transmitter, rectangular baseband pulses are directly multiplied with a carrier without pulse shaping.

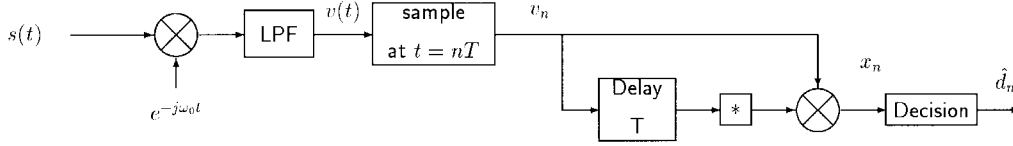


Fig. 1. Conventional DPSK receiver where  $\omega_0$  is the carrier frequency,  $T$  is the symbol period, and  $^{**}$  denotes the complex conjugate.

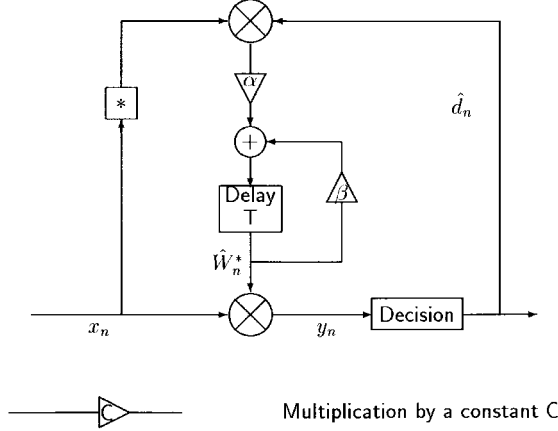


Fig. 2. The feedback-frequency drift compensator. Here  $x_n = d_n \cdot e^{j\Delta\omega T}$  in (1),  $\beta = 1 - \alpha$ , and  $^*$  denotes the complex conjugate.

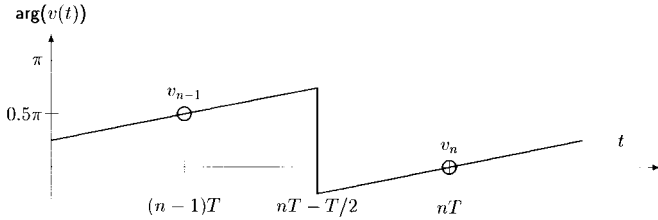


Fig. 3. The phase of  $v(t)$  when  $\theta_n - \theta_{n-1} = -\pi$ ,  $\Delta\omega T = 0.5\pi$ ,  $\theta_{n-1} = 0.5\pi$ , and  $\theta_0 = 0$ .

Then  $\theta(t)$  in (1) is constant over a symbol period  $[kT - T/2, kT + T/2]$ . It is expressed as

$$\theta(t) = \sum_k \alpha_k p_T(t - kT - T/2) \quad (5)$$

where  $p_T(t)$  is a rectangular pulse of support  $[0, T]$  with amplitude 1 and  $\alpha_n \in \{0, \pi\}$ . Again referring to Fig. 1,  $v(t)$  is given by

$$v(t) = e^{j\theta(t)} \cdot e^{j\Delta\omega t} \cdot e^{j\theta_0}. \quad (6)$$

The phase of  $x_n$  in Fig. 1 is

$$\arg(v_n) - \arg(v_{n-1}) = \theta_n - \theta_{n-1} + \Delta\omega T \quad (7)$$

where  $\arg(v_n)$  denotes the phase of  $v_n = v(nT)$ . Next, we show that the performance degradation caused by  $\Delta\omega T$  can be eliminated by considering boundary values of  $v(t)$  between symbol periods. The boundary values can be defined as  $b_n^i = \lim_{\epsilon \rightarrow 0} v(nT - T/2 + \epsilon)$  and  $b_n^f = \lim_{\epsilon \rightarrow 0} v(nT + T/2 - \epsilon)$  for  $\epsilon > 0$  where  $i$  and  $f$ , respectively, represent the initial and final values at the  $n$ th symbol period. The phase difference between  $b_n^i$  and  $b_{n-1}^f$  is expressed as

$$\begin{aligned} \arg(b_n^i) - \arg(b_{n-1}^f) &= \theta_n + \Delta\omega(nT - T/2) + \theta_0 - \theta_{n-1} \\ &\quad - \Delta\omega(nT - T/2) - \theta_0 \\ &= \theta_n - \theta_{n-1}. \end{aligned} \quad (8)$$

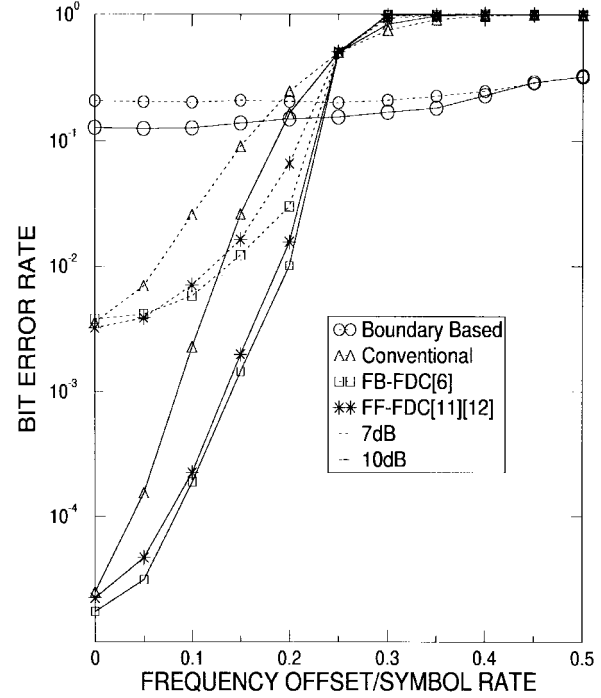


Fig. 4. Empirical BER values of the boundary-based detector, the conventional detector, the one with FB-FDC and the one with FF-FDC, where dotted and solid lines show the BER values when SNR is 7 and 10 dB, respectively.

Thus, the effect of the frequency shift is indeed removed. As an example, consider the phase of  $v(t)$  shown in Fig. 3 where  $\theta_n - \theta_{n-1} = -\pi$ ,  $\Delta\omega T = 0.5\pi$ ,  $\theta_{n-1} = 0.5\pi$ , and  $\theta_0 = 0$ . From this figure, we can see that  $\arg(v_n) - \arg(v_{n-1}) = -\pi/2$ , whereas  $\arg(b_n^i) - \arg(b_{n-1}^f) = -\pi$ .

Demodulation of DPSK signals using  $b_n^i$  and  $b_{n-1}^f$  would be a useful alternative to the conventional scheme in Fig. 1. These boundary values, however, cannot be obtained through direct sampling of  $v(t)$  at  $nT - T/2$ . They should be estimated from their neighboring values, which requires a sampling rate higher than the symbol rate  $1/T$ . We consider the sampling of  $v(t)$  at the Nyquist rate  $2/T$ . Let  $v_n^1$  and  $v_n^2$ , respectively, denote the samples of  $v(t)$  at  $t = nT - T/2 + t_0$  and  $t = nT + t_0$  for  $0 < t_0 < T/2$ . Estimates of  $b_n^i$  and  $b_n^f$  can be obtained by *least squares* estimation based on the *linear regression* model [10] using  $v_n^1$  and  $v_n^2$  values. Minimizing the least squares error  $\sum_{k=1}^2 [v_n^k - A(nT - T + kT/2 + t_0) + B]^2$  results in

$$A = (v_n^2 - v_n^1)/(T/2); \quad B = v_n^1 - (nT - T/2 + t_0)A. \quad (9)$$

This line  $At + B$  is merely the line connecting  $v_n^1$  and  $v_n^2$ . We can estimate  $b_n^i$  and  $b_n^f$  by putting  $t = nT - T/2$  and  $t = nT + T/2$  into  $At + B$ . The results are

$$\hat{b}_n^i = v_n^1 - At_0; \quad \hat{b}_n^f = 2v_n^2 - v_n^1 - At_0. \quad (10)$$

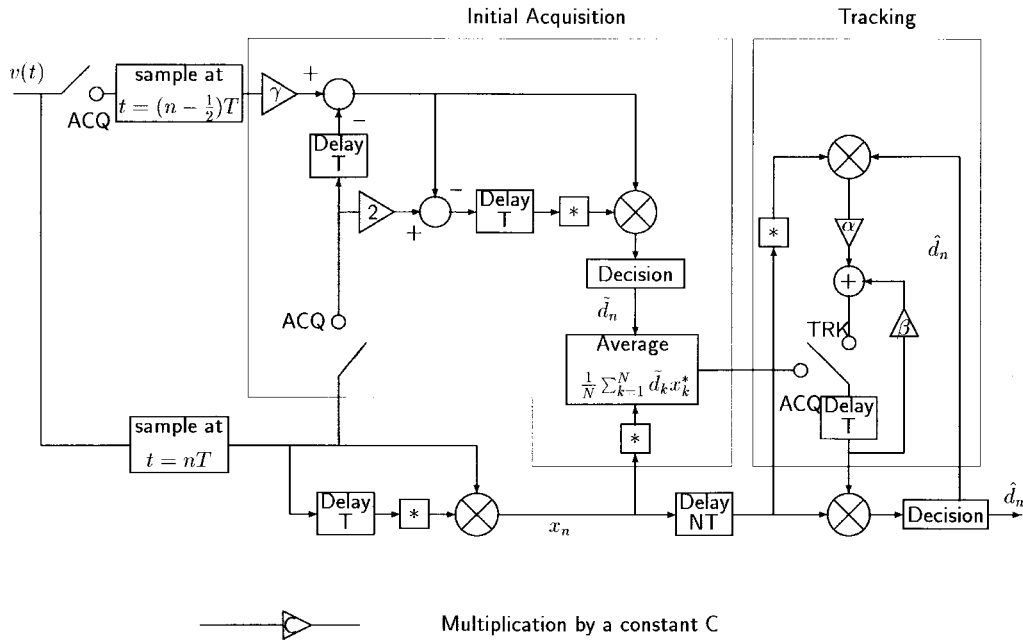


Fig. 5. Entire block diagram of the proposed DPSK demodulator, where  $\gamma = p(0.5T)^{-1}$ . When the roll-off factor is 0.5,  $\gamma = 1.667$ .

The DPSK demodulation technique using  $\hat{b}_n^i$  and  $\hat{b}_n^f$  values will be referred to as the *boundary-based* detection.

### B. Raised-Cosine Pulse Case

In practical communication systems, rectangular pulses are often converted into raised-cosine pulses having a bandlimited spectrum before transmission. For raised-cosine pulses, it is desirable to sample at  $nT$  because in the  $n$ th symbol period  $nT$  is the only position whose signal value is not corrupted by intersymbol interference (ISI) resulting from pulse shaping. Therefore, we sample  $v(t)$  at  $t = nT$  and  $t = nT - T/2$ . In this case, unlike the rectangular pulse case, we can sample at  $t = nT - T/2$  because a sharp transition between symbol periods does not exist. Note that  $t_0$  in (9) and (10) becomes zero. The sampled values, denoted by  $v_n^1 = v(nT - T/2)$  and  $v_n^2 = v(nT)$ , are expressed as

$$\begin{aligned} v_n^1 &= \sum_{k=-\infty}^{\infty} p((k-0.5)T) e^{j\theta_{n-k}} e^{j(\Delta\omega(n-0.5)T + \theta_0)} \\ v_n^2 &= e^{j(\theta_n + \Delta\omega nT + \theta_0)} \end{aligned} \quad (11)$$

where  $p(\cdot)$  is the impulse response of a raised-cosine pulse-shaping system. Obviously,  $v_n^2$  is not influenced by pulse shaping, and only the  $v_n^1$  value should be changed by removing ISI terms to get  $v_n^{1'}$  defined as  $e^{j(\theta_n + \Delta\omega(n-0.5)T + \theta_0)}$ . Based on the fact that  $p(0.5T)$  and  $p(-0.5T)$  cause dominant ISI terms,  $v_n^1$  is approximated as follows<sup>1</sup>:

$$\begin{aligned} v_n^1 &\approx p(0.5T) e^{j(\theta_{n-1} + \Delta\omega(n-0.5)T + \theta_0)} \\ &\quad + p(-0.5T) e^{j(\theta_n + \Delta\omega(n-0.5)T + \theta_0)}. \end{aligned} \quad (12)$$

<sup>1</sup>The expression in (12) is exact when the roll-off factor is 1.

Since  $p(0.5T) = p(-0.5T)$  and  $e^{j(\theta_{n-1} + \Delta\omega(n-0.5)T + \theta_0)} \approx v_{n-1}^2$ , we get

$$v_n^{1'} \approx \frac{v_n^1}{p(0.5T)} - v_{n-1}^2. \quad (13)$$

Following from (10), the boundary values for raised-cosine pulses are given by

$$\hat{b}_n^i = v_n^{1'}; \quad \hat{b}_n^f = 2v_n^2 - v_{n-1}^{1'}. \quad (14)$$

### C. Performance Evaluation of the Boundary-Based Detection

In order to evaluate the performance of the boundary-based detection, we generate *binary* DPSK symbols with 50% excess bandwidth raised-cosine pulse shaping (roll-off factor = 0.5). It was assumed that data were transmitted in short bursts of 105 symbols. A total of 15 000 bursts were generated and corrupted by additive white Gaussian noise (AWGN) and frequency shift. The corrupted bursts were passed through the boundary-based detector, and bit-error rate (BER) values were estimated by counting the number of errors in demodulating the 15 000 bursts. For comparison, the conventional DPSK receiver in Fig. 1, the one employing the FB-FDC in Fig. 2 ( $\alpha = 1/24$ ), and the method in [11] and [12] which estimates the frequency offset from the  $M$ th power of a baseband signal in  $M$ -ary DPSK were also considered. The frequency drift compensator based on the method in [11] and [12] will be referred to as *feedforward-FDC* (FF-FDC).

Fig. 4 shows the results of this simulation. It is seen that the boundary-based detector performs considerably worse than the others when the frequency shift  $\Delta f$  is small. This indicates that the former is vulnerable to AWGN. However, when  $\Delta f T > 0.2$ , the boundary-based detector outperformed the others; in fact, its BER looks almost constant irrespective of  $\Delta f T$ . This result suggests that the boundary-based detector can be effective for initial acquisition of  $\Delta f$ .

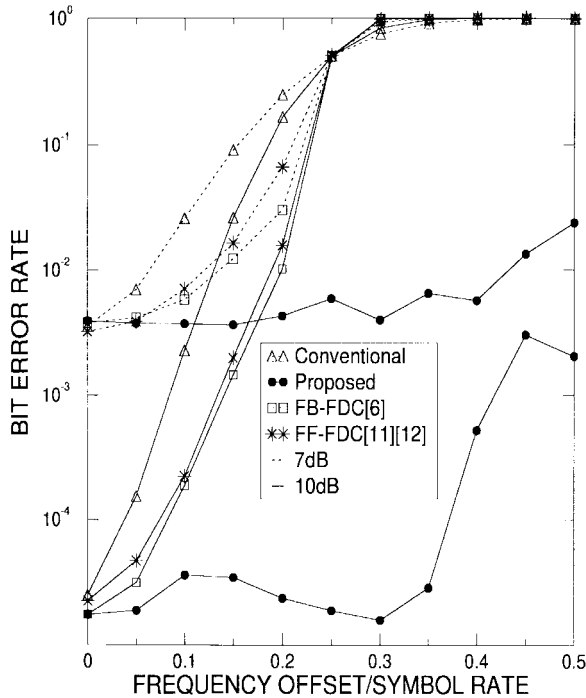


Fig. 6. Empirical BER values of the conventional detector, the one with FB-FDC, the one with FF-FDC and the proposed detector, where dotted and solid lines show the BER values when SNR is 7 and 10 dB, respectively.

#### IV. THE PROPOSED DPSK DETECTOR

##### A. The Algorithm

The demodulation scheme proposed in this section incorporates the boundary-based detection with the FB-FDC. Its entire block diagram is illustrated in Fig. 5. At the beginning, the switches in Fig. 5 are connected to the ACQ positions, and the initial value of  $\hat{W}_n^*$  in (4), denoted by  $\hat{W}_0^*$ , is determined by using the boundary-based detector. Assuming that a total of  $L$  DPSK symbols are transmitted, the procedure is stated as follows.

- 1) Sample  $2N$  values at Nyquist rate over the first  $N$  symbol periods. Here,  $N \ll L$ .
- 2) Apply the boundary-based detector to get an estimate of  $d_n$  defined in (2). This estimate is called the *tentative* estimate of  $d_n$ , and is denoted by  $\tilde{d}_n$ .
- 3) Since  $d_n x_n^* = e^{-j\Delta\omega T}$  from (2), we evaluate  $(1/N) \sum_{k=1}^N \tilde{d}_k x_k^*$  and use this value as  $\hat{W}_0^*$ .

After obtaining  $\hat{W}_0$ , the two switches in Fig. 5 providing data to the initial acquisition part are open, and the one in the tracking part is connected to the TRK position. Then this system becomes the DPSK demodulator employing the FB-FDC with the initial value  $\hat{W}_0$ . This demodulation scheme is

applied to the entire sequence sampled at  $nT$ ,  $n = 1, \dots, L$ . The “delay  $NT$ ” block in Fig. 5 is required to store the first  $N$  data which have been used for acquisition. Final output is the estimated sequence  $\hat{d}_n$ ,  $n = 1, \dots, L$ . Note that the tentative decision values  $\tilde{d}_n$ ,  $n = 1, \dots, N$  obtained during acquisition are replaced with  $\hat{d}_n$ .

##### B. Performance Evaluation of the Proposed Detector

Inputs to the demodulator were generated as in Section III-C. Empirical BER values were evaluated for the proposed demodulator, the conventional one, the one with the FB-FDC, and the one with FF-FDC. We set  $N = 32$  and  $\alpha = 1/24$ . The results shown in Fig. 6 demonstrate that the proposed scheme can outperform the others for all  $\Delta f T$  values, and is indeed robust to frequency shift.

#### V. CONCLUSION

A new DPSK demodulation scheme which is robust to frequency shift was proposed, and its performance was examined through computer simulation. This method performed better than existing techniques in [6] and [11] at the expense of higher sampling rate and some additional computation. The proposed scheme is particularly useful in applications where transmission is affected by large frequency shifts.

#### REFERENCES

- [1] J. H. Park Jr., “On binary DPSK detection,” *IEEE Trans. Commun.*, vol. COM-26, pp. 484–486, Apr. 1978.
- [2] N. M. Blachman, “The effect of phase error on DPSK error probability,” *IEEE Trans. Commun.*, vol. COM-29, pp. 364–365, Mar. 1981.
- [3] R. F. Pawula, S. O. Rice, and J. H. Roberts, “Distribution of the phase angle between two vectors perturbed by Gaussian noise,” *IEEE Trans. Commun.*, vol. COM-30, pp. 1828–1841, Aug. 1982.
- [4] F. D. Natali, “AFC tracking algorithms,” *IEEE Trans. Commun.*, vol. COM-32, pp. 935–947, Aug. 1984.
- [5] M. K. Simon and D. Divsalar, “Doppler-corrected differential detection of MPSK,” *IEEE Trans. Commun.*, vol. 37, pp. 99–109, Feb. 1989.
- [6] M. Ikura *et al.*, “Baseband processing frequency-drift-compensation for QDPSK signal transmission,” *Electron. Lett.*, vol. 27, pp. 1521–1523, Aug. 1991.
- [7] M. Ikura *et al.*, “Baseband-processing feedforward carrier frequency drift compensation for DPSK mobile radio,” *Electron. Lett.*, vol. 28, pp. 771–773, Apr. 1992.
- [8] M. Ikura and F. Adachi, “Baseband feedforward frequency drift compensation without false phase locking for burst DPSK signal reception,” *Electron. Lett.*, vol. 28, pp. 1165–1167, June 1992.
- [9] S. Haykin, *Adaptive Filter Theory*. Englewood Cliffs, NJ: Prentice-Hall, 1991.
- [10] P. J. Bickel and K. A. Doksum, *Mathematical Statistics: Basic Ideas and Selected Topics*. San Francisco, CA: Holden-Day, 1977.
- [11] E. Biglieri, F. Avrishkamar, and Y. C. Jou, “Doppler frequency shift estimation for differentially coherent CPM,” *IEEE Trans. Commun.*, vol. 38, pp. 1659–1663, Oct. 1990.
- [12] N. Hamamoto, “Differential detection with IIR filter for improving DPSK detection performance,” *IEEE Trans. Commun.*, vol. 44, pp. 959–966, Aug. 1996.